HHS Public Access

Author manuscript

Biochim Biophys Acta. Author manuscript; available in PMC 2017 July 01.

Published in final edited form as:

Biochim Biophys Acta. 2016 July ; 1861(7): 671–679. doi:10.1016/j.bbalip.2016.04.014.

Two functionally distinct pools of eNOS in endothelium are facilitated by myoendothelial junction lipid composition

Lauren A. Biwer[1,2], **Evan P. Taddeo**[3], **Brandon M. Kenwood**[3], **Kyle L. Hoehn**[3,4], **Adam C. Straub**[5,6], and **Brant E. Isakson**[1,2]

[1]Department of Molecular Physiology and Biophysics, University of Virginia

[2]Robert M. Berne Cardiovascular Research Center, University of Virginia

[3]Department of Pharmacology at University of Virginia

[4]School of Biotechnology and Biomolecular Sciences, University of New South Wales, Australia

[5]Department of Pharmacology and Chemical Biology, University of Pittsburgh

[6]Heart, Lung, Blood and Vascular Medicine Institute; University of Pittsburgh

Abstract

In resistance arteries, endothelial cells (EC) make contact with smooth muscle cells (SMC), forming myoendothelial junctions (MEJ). Endothelial nitric oxide synthase (eNOS) is present in the luminal side of the EC (apical EC) and the basal side of the EC (MEJ). To test if these eNOS pools acted in sync or separately, we co-cultured ECs and SMCs, then stimulated SMCs with phenylephrine (PE). Adrenergic activation causes inositol (1,4,5) triphosphate (IP_3) to move from SMC to EC through gap junctions at the MEJ. PE increases MEJ eNOS phosphorylation (eNOS-P) at S1177, but not in EC. Conversely, we used bradykinin (BK) to increase EC calcium; this increased EC eNOS-P but did not affect MEJ eNOS-P. Inhibiting gap junctions abrogated the MEJ eNOS-P after PE, but had no effect on BK eNOS-P. Differential lipid composition between apical EC and MEJ may account for the compartmentalized eNOS-P response. Indeed, DAG and phosphatidylserine are both enriched in MEJ. These lipids are cofactors for PKC activity, which was significantly increased at the MEJ after PE. Because PKC activity also relies on endoplasmic reticulum (ER) calcium release, we used thapsigargin and xestospongin C, BAPTA, and PKC inhibitors, which caused significant decreases in MEJ eNOS-P after PE. Functionally, BK inhibited leukocyte adhesion and PE caused an increase in SMC cGMP. We hypothesize that local

To whom correspondence should be addressed: Brant Isakson, Robert M Berne Cardiovascular Research Center, University of Virginia School of Medicine, P.O. Box 801394, Charlottesville, VA 22908, Telephone (434) 924-2093; Fax (434) 924-2828; brant@virginia.edu.

Conflict of Interest: The authors declare that they have no conflicts of interest with the contents of this article.

Author contributions: LAB conducted experiments, analyzed results and wrote most of the paper. ET and BK helped with experiment conception, conducted lipid experiments and helped with data analysis. KH helped with experiment conception, data analysis and editing of the paper. ACS conducted experiments, analyzed results and edited the paper. BEI helped with data analysis, editing the paper and supporting the work.

lipid composition of the MEJ primes PKC and eNOS-P for stimulation by PE, allowing for compartmentalized function of eNOS in the blood vessel wall.

Graphical Abstract

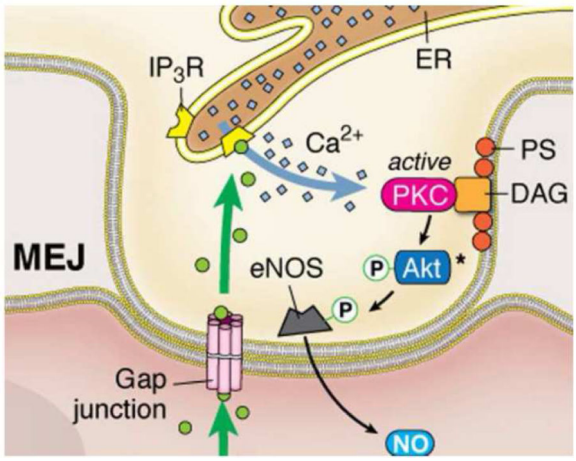

Keywords

endothelial cell; nitric oxide synthase; endoplasmic reticulum; protein kinase C; diacylglycerol; microcirculation; myoendothelial junction

INTRODUCTION

Endothelial nitric oxide synthase (eNOS) is one of the most important enzymes found in endothelial cells (EC) that line the lumen of arteries and veins. Its ability to generate nitric oxide (NO) allows for control of vascular tone along with preventing inflammation and proliferation of the surrounding vascular smooth muscle cells (SMC)(1–3). Alterations in eNOS activity or expression are linked to a number of cardiovascular pathologies that exhibit endothelial dysfunction, such as hypertension and inflammation (4,5).

Localization of eNOS within the EC has been shown in the perinuclear region (Golgi) and at the plasma membrane in vitro (6) and in vivo (7). Targeting eNOS to these domains requires lipid modifications such as acylation (8). These cellular regulatory processes are important as deviation from normal localization or modification renders eNOS unable to increase its activation via phosphorylation (6). Under unstimulated circumstances, eNOS is sequestered in specialized lipid domains at the plasma membrane, which are characterized by the presence of cholesterol and caveolae, flask-shaped invaginations of the plasma membrane (8). The coat protein of caveolae, caveolin 1, directly interacts with eNOS to maintain its quiescence (9,10). However, increases in intracellular calcium ($[Ca^{2+}]_i$), cause membrane dissociation and subsequent translocation to the cytosol. Enzyme phosphorylation is increased at one of several activating sites, including S1177 in human EC, causing the production of NO.

Importantly, the myoendothelial junction (MEJ) has been shown to be a source of phosphorylated, activated eNOS that generates NO, regulating heterocellular communication and vascular tone (11–13). The MEJ is a cellular projection, typically endothelial in origin, that allows for direct cytoplasmic contact with the smooth muscle cells that comprise the outer wall of small diameter arteries and arterioles (14). After stimulation of α_{1D}-adrenergic receptors on SMC with phenylephrine (PE), inositol (1,4,5) triphosphate (IP_3) can travel through MEJ-localized gap junctions and induce endoplasmic reticulum (ER) calcium release via local IP_3 receptor (IP_3R) expression (15–17), which increases EC production of NO (18) via eNOS phosphorylation at serine 1177 (eNOS-P)(19). Given the function of eNOS as a regulator of normal and pathological vascular physiology, we wanted to investigate the distinct subcellular characteristics and function of eNOS in EC that form MEJs. Using an *in vitro* vascular cell co-culture (VCCC) model, we show that there are two distinct pools of eNOS in the endothelium that are differentially activated. This has different functional consequences, which may be due to differences in lipid composition, along with protein kinase C (PKC) localization and activity at the MEJ.

MATERIALS & METHODS

VCCC

Primary coronary artery human endothelial cells and smooth muscle cells (Lonza) were cultured and plated on opposing sides of transwell filters. This culture model system allows EC and SMC to be cultured as individual monolayers, but make physical contact at discrete in vitro MEJs within the pores of transwell insert (as extensively described by (11,13,15,20,21)). Pharmacological compounds were added to the media except where noted. Bradykinin (10μM), L-NAME (100μM), TNFα (10ng/mL), Gö-6976 /Gö-6983 (10μM), BAPTA (20μM), Thapsigargin (2μM) and Xestospongin C (20μM) were all added to the EC side. PE (50μM) was added to the SMC side. The gap junction inhibitor 18-GA (50μM), the NO donor GSNO (100μM) were added to both EC and SMC.

Immunofluorescence

Transverse sections of the VCCC filter were fixed in 4% PFA, transversely embedded in paraffin and sectioned. Slides were incubated overnight with antibodies to alpha 1 adrenergic receptor (Santa Cruz), bradykinin receptor 2 (Abcam), total eNOS, S1177 eNOS (BD Bioscience), or calreticulin (Thermo-Fisher).

Western Blotting

The VCCC fractions (EC/MEJ/SMC) were scraped in 1× PBS and placed in lysis buffer as previously described (13,20). Then EC/MEJ/SMC fractions were sonicated and subjected to electrophoresis as described (20). Briefly, SMC were thoroughly scraped from one side and EC were thoroughly scraped off the other side. The remaining protein and membranes within the filter pores of the transwell are considered the MEJ fraction; the whole filter was immersed in protein lysis buffer after removal of EC and SMC. Then EC/MEJ/SMC fractions were sonicated and subjected to electrophoresis as described (20). Blots were probed for S1177 eNOS, stripped and reprobed for total eNOS. Band intensities were

quantified using Li-Cor Odyssey Image Studio Software and values for S1177 eNOS were normalized to total eNOS.

Measurement of Glycerolipids, Phospholipid Derivatives and Sphingolipids

VCCC fractions and the filter were harvested in 1× PBS without addition of protein lysis buffer. Phospholipid derivatives and sphingolipids were extracted and quantified by liquid chromatography-mass spectrometry, as previously described (22) with the following modifications. Extracted glycerolipids and phospholipids were resuspended in methanol:chloroform:millipure H_2O (4:1:1) and analyzed after separation with a Kinetex C18 column. Mobile phase A consisted of 60% acetonitrile, 40% H_2O, 0.1% formic acid and 1mM ammonium formate. Mobile phase B consisted of 90% isopropanol, 10% acetonitrile, 0.1% formic acid, and 1mM ammonium formate. Total flow rate was 0.8mL/min. Sphingolipid extracts were divided in half for the analysis of ceramides and sphingosine-1-phosphate (S1P) species. For ceramide measurements, 500μL of chloroform and 1mL of millipure H_2O were added to each sample. Extracts were vortexed and centrifuged at 2000rpm for 10min. The organic phase was isolated, dried down under N_2 and resuspended in 97% acetonitrile, 2% methanol, 1% formic acid (v/v/v) with 5mM ammonium formate. For S1Ps, one half of the sphingolipid extract was centrifuged at maximum speed for 10min, and the supernatant was dried down and resuspended in methanol. Both ceramides and S1Ps were analyzed by liquid chromatography-mass spectrometry following previously established methods (23). Values were normalized to an internal standard and then to protein concentration. For measurement of cholesterol, total lipids were extracted from the VCCC using an adapted Folch method as previously described (24). Samples were then assayed for total cholesterol using the fluorometric Amplex Red Cholesterol Assay kit (Thermo Fisher). Background fluorescence was subtracted from the initial fluorescent value.

PKC assay

Each of the VCCC fractions were stimulated with PE or no treatment for 1 minute, then harvested into lysis buffer and ran in triplicate (5ug lysate/well) following the assay protocol and recommended lysis buffer (Abcam). Background absorbance was subtracted from the initial values, then normalized to protein concentration and presented as relative activity.

Static adhesion assay

Leukocyte adhesion to the EC of the VCCC was performed by co culturing human umbilical vein endothelial and smooth muscle cells on the opposing sidesof transwell inserts. THP1 monocytes were grown separately in RPMI media without antibiotics. Before addition to the VCCC, the monocytes were loaded with 5μM calcein AM for 20 minutes in Krebes-Hepes. Four hours before harvest, all transwells (except control) were incubated with TNF-α in Krebs-Hepes buffer. BK, PE and GSNO were added after four hours of TNF-α. After 1 minute of agonist stimulation, calcein loaded THP1 monocytes were added to the EC side of the VCCC for 5 minutes. Cells were then gently washed with Krebs-Hepes and fixed with 4%PFA for 20 minutes. The transwell filter was excised and mounted on a slide and adherent leukocytes were quantified.

Cyclic GMP assay

Cyclic GMP was determined according to kit instructions (Cell Signaling) and as previously described (12,13).

Statistics

One way analysis of variance was used with Tukey post-test or Dunnett's multiple comparison post-test.

RESULTS

We have previously demonstrated differential pools of eNOS in EC of resistance arteries: in the apical EC and at the portion of the EC making contact with the SMC, the MEJ (11). These two areas of EC are physically distinct and an accumulation of evidence has now demonstrated that these two areas are also functionally distinct (13,15,25). Because NO generation in EC must be tightly regulated, we hypothesized that eNOS activation, as demonstrated by eNOS phosphorylation at serine (S)1177 (eNOS-P), may occur locally. To test this concept, we utilized our well-described VCCC (15,20,21) that crucially has EC directly linked to SMC by EC-derived MEJs via gap junctions (Figure 1A).

eNOS phosphorylation at S1177

In an attempt to selectively activate eNOS, we first wanted to ensure receptors for EC or SMC agonists were only found in each cell type. Using immunocytochemistry, we found that BK receptor 2 was only found on EC and α_{1D}-adrenergic receptors were only found on SMC, with eNOS found in both apical EC and at the MEJ (Figure 1A). To test that we could induce eNOS phosphorylation in either apical EC or MEJ, we found that 1 minute after stimulation with either BK or PE increased eNOS-P that appeared to be either apical or MEJ in nature (Figure 1B). Although there was some staining in the EC monolayer after PE stimulation in Figure 1B, it was not as punctate as that seen in the holes of the transwell where the in vitro MEJs are located. Next, we performed western blot analysis on each of the fractions from the VCCC and found that after BK stimulation, only apical EC could demonstrate an increase in eNOS phosphorylation and this was not evident at the MEJ (Figure 1C). However, after PE stimulation, an increase in MEJ eNOS phosphorylation occurred without a change in apical EC (Figure 1D).

Because an increase in $[Ca^{2+}]_i$ alone can regulate eNOS phosphorylation, we pretreated both EC and SMC with the gap junction inhibitor 18-GA; this selectively inhibited eNOS phosphorylation at the MEJ after PE stimulation (Figure 2B), but not in apical EC after bradykinin stimulation (Figure 2A). Therefore, it appears that depending on whether EC or SMC is stimulated, eNOS is activated in distinct locations of the EC.

Lipid composition and PKC activity

Next, we wanted to understand how EC could selectively allow for eNOS phosphorylation in the apical or MEJ regions of the cell. Because the MEJ itself has been shown to be a unique signaling microdomain and has a highly curved physical structure, we assessed lipid composition of the cells in the VCCC and compared them to unpolarized EC and SMC from

a single monolayer (Table 1). We found phospholipid composition of EC or SMC in co-culture has a unique profile, rendering it profoundly different from a monolayer of the same cells. There were no significant differences in structural lipids phosphatidylcholine, phosphatidylethanolamine or sphingomyelin at the MEJ, but cholesterol content at the MEJ was significantly decreased (Table 1). Ceramide has been shown to activate eNOS phosphorylation via a calcium-independent pathway (26), however the ceramide levels at the MEJ are not significantly different from the rest of the EC (Table 1). Moreover, the signaling lipid sphingosine-1-phosphate (S1P) has also been shown to activate eNOS via its receptors on vascular cells (27,28). MEJ levels of S1P were significantly lower than the rest of the EC (Table 1), but S1P signaling and expression or function of S1P receptors at the MEJ has not been investigated. When phosphatidylserine (PS) and diacylglycerol (DAG), direct lipid cofactors for PKC activity, were analyzed, we found them to be significantly enriched at the MEJ (Figure 3A, 3B). Concomitant with these results, we found PKC activity is significantly higher at the MEJ, and further increases after PE stimulation (Figure 3C).

Calcium dependent MEJ eNOS phosphorylation

In addition to DAG and PS, conventional isoforms of PKC require IP_3 stimulated calcium release for activation (29,30). The ER has been shown to be present at MEJ and is possibly an important component to the negative feedback of SMC induced constriction (15,16). Not surprisingly, the VCCC also was found to have expression of the ER marker calreticulin in EC, MEJ and SMC (Figure 4A, B). In order to demonstrate a possible role for the calcium sequestered in these ER projections on eNOS-P at the MEJ, the VCCC were incubated with BAPTA-AM and then stimulated with PE. This almost completely blocked MEJ eNOS-P (a 92% decrease). After stimulation with PE, ER calcium release contributes to eNOS-P at the MEJ as thapsigargin and xestospongin C significantly decreased eNOS-P. Importantly, the broad spectrum PKC inhibitor Gö-6983 significantly decreased MEJ eNOS-P after PE while the conventional isoform inhibitor Gö-6976 only trended in that direction (Figure 4C). Entire blots for each antibody are demonstrated in Supplementary Figure 1.

Functional contribution of differential activatable pools of eNOS in endothelium

Based on the work above, it was clear that ECs tightly regulate eNOS activation either apically or at the MEJ, depending on the stimulus. However, it was unclear to what extent this may differentially regulate the functional effect of eNOS. It is well known that NO is a potent inhibitor of leukocyte adhesion to inflamed endothelial cells (1) so we hypothesized the apical eNOS, regulated by BK stimulation, could selectively affect the ability of monocytes to adhere to the EC. To test this, we used the pro inflammatory cytokine TNF-α to initiate leukocyte adhesion to the EC layer of the VCCC and activated the different pools of eNOS with BK or PE. Adding TNF-α significantly increased adhesion of the calcein-loaded THP1 monocytes compared to control (Figure 5A). Inhibiting eNOS with L-NAME significantly exacerbated adhesion compared to TNF-α alone. Stimulation of EC with BK significantly decreased the degree of leukocyte adhesion which is consistent with localized eNOS activation and NO release. However, adding PE had no effect on leukocyte adhesion, consistent with the differences in localized eNOS phosphorylation observed above. Therefore, apical eNOS appears to be distinctly important in abrogating leukocyte adhesion, whereas as MEJ eNOS does not appear to have an effect.

In order to determine a functional role for the eNOS at the MEJ, we examined SMC cGMP production, which is generated after NO binds to soluble guanyl cyclase. We hypothesized that MEJ localized eNOS and its proximity to the SMC made it a much better regulator of SMC dilation than eNOS in the apical portion of EC. Application of PE caused a significant increase in cGMP production after 5 minutes in SMC (Figure 5C) that is abrogated in the presence of gap junction inhibition (Figure 5D). This is in line with the eNOS-P observed above. Importantly, cGMP production does not occur in SMC grown in a monolayer without MEJ formation (Figure 5E), underscoring the importance of the MEJ localized eNOS phosphorylation event.

DISCUSSION

In this paper, we have shown the presence of two functionally distinct sources of eNOS in the endothelium. Despite the apical and MEJ eNOS similarity in basal levels of phosphorylation, they are activated differently depending on agonist stimulation. Based on the data presented, this may be due to differences in membrane lipid composition and kinase activity at the MEJ, which is underscored by the contribution of ER calcium. While the spatial localization of eNOS in the endothelium may have divergent functions (i.e. leukocyte adhesion versus production of SMC cGMP), this could be explained by the ability of the cellular microenvironment to control differential eNOS activation, thereby providing another level of NO control in the vascular wall (Figure 6).

Specific protein localization to the MEJ is important for cellular signaling and eNOS is a central mediator of signaling processes at the MEJ (31). Our lab has previously shown that MEJ-localized eNOS participates in S-nitrosylation of connexin 43 and this allows the heterocellular transfer of small signaling molecules such as IP_3 (11). Connexins (Cx) at cellular borders can also influence eNOS localization. Under normal cell conditions, Cx40 and Cx37 interact with eNOS (32,33), but connexin 40 knockout mice have decreased aortic eNOS expression (34). Although aortas have very few MEJs, the possibility that Cx may dictate eNOS localization in smaller diameter arteries with more MEJs could provide an explanation for the two spatial distinct pools of eNOS. Indeed, both Cx40 and Cx37 have been directly localized to MEJs (35).

In addition to its ability to post-translationally modify proteins at the MEJ, we have shown that eNOS directly interacts with alpha hemoglobin to regulate NO diffusion at the MEJ (12,13). The localized presence of organelles such as peripheral ER with a thapsigargin/xestospongin C sensitive pool of calcium regulate the signaling processes at the MEJ by activating PKC and eNOS (Figure 4). The unique tubular structure of the peripheral ER (36) allows for projection into the MEJ and local calcium release. IP_3R localization at the MEJ (15,17) facilitates the SMC to EC signaling cascade after PE stimulation of the α_{1D}-adrenergic receptor.

The subcellular localization of eNOS is strategically determined by the EC as the magnitude of eNOS activity is dependent on where the enzyme is present. For example, nuclear directed eNOS is significantly less phosphorylated (37), while eNOS targeted to the plasma membrane generates the most NO, likely via its close association to membrane bound

kinases (38). As eNOS-generated NO is a small gaseous molecule that can act in a local manner (37), it corresponds that eNOS would be preferentially targeted to signaling microdomains such as the MEJ. This allows for interaction with distinct protein partners that can regulate divergent physiological functions.

Basal eNOS phosphorylation occurs at both the apical EC and at the MEJ (11). In bovine EC, eNOS can be regulated by dual phosphorylation at the S635 and S1179 residues (38), which indicates there may be other modifications of serine or threonine sites on MEJ eNOS after PE, as we solely focused on S1177 phosphorylation. Fleming et al has shown bradykinin stimulation of the EC resulted in rapid increases of S1177 phosphorylation and T495 dephosphorylation. These particular events were not influenced by the addition of PKC inhibitors but instead were dependent on the activity of calcium/calmodulin kinase II (39). Presumably, this process is occurring in the apical EC as the MEJ eNOS does not increase phosphorylation in response to bradykinin and is regulated in part by PKC.

While PKC can be distributed throughout the cell, it has the ability to localize into subcellular signaling microdomains (40,41). Only one paper has noted the presence of any PKC isoform at the MEJ, and PKC itself was not the focus of that paper (42). There is precedent for PKC regulation of eNOS phosphorylation (43–46) and the phosphorylation of eNOS being dependent on ER-derived calcium (47). The MEJ lipidomic results presented here point to, for the first time, 1) an ideal lipid environment for PKC based on the enrichment of PS and DAG and 2) a unique lipid environment in this arterial model as compared to EC and SMC grown in alone and in non-polarized conditions.

Using the pan-PKC inhibitor, Gö-6983, we observe a significant reduction in S1177 eNOS phosphorylation at the MEJ. Based on previous work, it has been reported that PKCα can specifically phosphorylate eNOS on S1177 (44,48) and likely contributes to eNOS phosphorylation at the MEJ In addition, it is possible the PKCα may act upstream of Akt, a kinase that has been shown to directly phosphorylate eNOS; studies have shown that PKCα activity influences AKT phosphorylation and activity (44,49,50). Regardless, the enrichment of PS and DAG provide the key substrates for PKCα-AKT regulated eNOS phosphorylation providing another level of localized and controlled NO release to regulate specific functions in the vessel wall. While there are currently no studies to support this idea, experiments designed to modulate the lipid composition of co-cultured ECs and SMCs could lend support to the idea that lipids at the MEJ are essential for local NO signaling and heterocellular signaling in resistance arteries.

The lipid composition of cellular membranes can facilitate both the curvature of cellular projections (i.e. the MEJ) and cellular signaling via bioactive lipids or assembly of proteins and receptors important for signaling. Cholesterol content has never been investigated at the MEJ, and we found that it was significantly lower than EC cholesterol (Table 1). The cell exhibits regional differences in cholesterol expression (51) and cholesterol provides rigidity to membranes by packing tightly with saturated sphingolipids (52), which would be an impediment to the dynamic extension and retraction that the MEJ exhibits (14). Intracellular membranes (like that of the ER) also have very low amounts of cholesterol and the cholesterol generated in the ER is exported rapidly to other organelles (53). Therefore the

enrichment of ER at the MEJ could “dilute” the concentration of cholesterol that we measured. Another plausible reason may be to enhance NO diffusion to SMC-localized soluble guanylate cyclase; increased amounts of cholesterol inhibit NO diffusion through membranes (54).

This study focuses on *in vitro* model of the MEJ, a system that although appears to reliably reproduces many characteristics of the MEJ that are seen *in viv*o, is still not an intact blood vessel wall. In addition, the entirety of this study was conducted in human primary endothelial and smooth muscle cells, which may have taken on conditions different than the intact blood vessel. This gives us caution when extrapolating our results to the intact MEJ. However, investigating the MEJ in isolation for proteomic analysis via an intact artery is currently not possible in this context. Further work in this area could help validate some of these initial results presented on lipid dynamics.

In summary, we have shown PE stimulation of SMC leads to MEJ specific eNOS phosphorylation while BK stimulation of EC only affects the apical pool of eNOS. These distinct pools exhibit differential effects of NO on the EC or SMC, owing to the unique lipid composition of the MEJ, localized ER and PKC activity. There is a strong possibility that the eNOS sequestration and selective activation in other polarized cell systems due to lipid membrane composition could also give rise to localized NO generation and function.

Supplementary Material

Refer to Web version on PubMed Central for supplementary material.

Acknowledgments

We thank the University of Virginia Histology Core for processing and sectioning of the VCCC and Anita Impagliazzo for the illustration. LAB was supported by AHA predoctoral fellowship 14PRE20420024, ACS by NIH HL112904-02 and BEI by NIH P01/R01.

REFERENCES

1. Kubes P, Suzuki M, Granger DN. Nitric oxide: an endogenous modulator of leukocyte adhesion. Proceedings of the National Academy of Sciences of the United States of America. 1991; 88:4651–4655. [PubMed: 1675786]
2. Shu X, Keller TCt, Begandt D, Butcher JT, Biwer L, Keller AS, Columbus L, Isakson BE. Endothelial nitric oxide synthase in the microcirculation. Cellular and molecular life sciences : CMLS. 2015
3. Forstermann U, Sessa WC. Nitric oxide synthases: regulation and function. European heart journal. 2012; 33:829–837. 837a–837d. [PubMed: 21890489]
4. Heiss C, Rodriguez-Mateos A, Kelm M. Central role of eNOS in the maintenance of endothelial homeostasis. Antioxidants & redox signaling. 2015; 22:1230–1242. [PubMed: 25330054]
5. Shesely EG, Maeda N, Kim HS, Desai KM, Krege JH, Laubach VE, Sherman PA, Sessa WC, Smithies O. Elevated blood pressures in mice lacking endothelial nitric oxide synthase. Proceedings of the National Academy of Sciences of the United States of America. 1996; 93:13176–13181. [PubMed: 8917564]
6. Fulton D, Fontana J, Sowa G, Gratton JP, Lin M, Li KX, Michell B, Kemp BE, Rodman D, Sessa WC. Localization of endothelial nitric-oxide synthase phosphorylated on serine 1179 and nitric oxide in Golgi and plasma membrane defines the existence of two pools of active enzyme. The Journal of biological chemistry. 2002; 277:4277–4284. [PubMed: 11729179]

7. van Haperen R, Cheng C, Mees BM, van Deel E, de Waard M, van Damme LC, van Gent T, van Aken T, Krams R, Duncker DJ, de Crom R. Functional expression of endothelial nitric oxide synthase fused to green fluorescent protein in transgenic mice. The American journal of pathology. 2003; 163:1677–1686. [PubMed: 14507674]
8. Shaul PW, Smart EJ, Robinson LJ, German Z, Yuhanna IS, Ying Y, Anderson RG, Michel T. Acylation targets emdothelial nitric-oxide synthase to plasmalemmal caveolae. The Journal of biological chemistry. 1996; 271:6518–6522. [PubMed: 8626455]
9. Ju H, Zou R, Venema VJ, Venema RC. Direct interaction of endothelial nitric-oxide synthase and caveolin-1 inhibits synthase activity. The Journal of biological chemistry. 1997; 272:18522–18525. [PubMed: 9228013]
10. Michel JB, Feron O, Sacks D, Michel T. Reciprocal regulation of endothelial nitric-oxide synthase by Ca2+-calmodulin and caveolin. The Journal of biological chemistry. 1997; 272:15583–15586. [PubMed: 9188442]
11. Straub AC, Billaud M, Johnstone SR, Best AK, Yemen S, Dwyer ST, Looft-Wilson R, Lysiak JJ, Gaston B, Palmer L, Isakson BE. Compartmentalized connexin 43 s-nitrosylation/denitrosylation regulates heterocellular communication in the vessel wall. Arteriosclerosis, thrombosis, and vascular biology. 2011; 31:399–407.
12. Straub AC, Butcher JT, Billaud M, Mutchler SM, Artamonov MV, Nguyen AT, Johnson T, Best AK, Miller MP, Palmer LA, Columbus L, Somlyo AV, Le TH, Isakson BE. Hemoglobin alpha/eNOS coupling at myoendothelial junctions is required for nitric oxide scavenging during vasoconstriction. Arteriosclerosis, thrombosis, and vascular biology. 2014; 34:2594–2600.
13. Straub AC, Lohman AW, Billaud M, Johnstone SR, Dwyer ST, Lee MY, Bortz PS, Best AK, Columbus L, Gaston B, Isakson BE. Endothelial cell expression of haemoglobin alpha regulates nitric oxide signalling. Nature. 2012; 491:473–477. [PubMed: 23123858]
14. Heberlein KR, Straub AC, Isakson BE. The myoendothelial junction: breaking through the matrix? Microcirculation. 2009; 16:307–322. [PubMed: 19330678]
15. Isakson BE. Localized expression of an Ins(1,4,5)P3 receptor at the myoendothelial junction selectively regulates heterocellular Ca2+ communication. Journal of cell science. 2008; 121:3664–3673. [PubMed: 18946029]
16. Isakson BE, Ramos SI, Duling BR. Ca2+ and inositol 1,4,5-trisphosphate-mediated signaling across the myoendothelial junction. Circulation research. 2007; 100:246–254. [PubMed: 17218602]
17. Toussaint F, Charbel C, Blanchette A, Ledoux J. CaMKII regulates intracellular Ca(2+) dynamics in native endothelial cells. Cell calcium. 2015; 58:275–285. [PubMed: 26100947]
18. Dora KA, Doyle MP, Duling BR. Elevation of intracellular calcium in smooth muscle causes endothelial cell generation of NO in arterioles. Proceedings of the National Academy of Sciences of the United States of America. 1997; 94:6529–6534. [PubMed: 9177252]
19. Looft-Wilson RC, Todd SE, Araj CA, Mutchler SM, Goodell CA. Alpha(1)-adrenergic-mediated eNOS phosphorylation in intact arteries. Vascular pharmacology. 2013; 58:112–117. [PubMed: 22982055]
20. Heberlein KR, Straub AC, Best AK, Greyson MA, Looft-Wilson RC, Sharma PR, Meher A, Leitinger N, Isakson BE. Plasminogen activator inhibitor-1 regulates myoendothelial junction formation. Circulation research. 2010; 106:1092–1102. [PubMed: 20133900]
21. Isakson BE, Duling BR. Heterocellular contact at the myoendothelial junction influences gap junction organization. Circulation research. 2005; 97:44–51. [PubMed: 15961721]
22. Taddeo EP, Laker RC, Breen DS, Akhtar YN, Kenwood BM, Liao JA, Zhang M, Fazakerley DJ, Tomsig JL, Harris TE, Keller SR, Chow JD, Lynch KR, Chokki M, Molkentin JD, Turner N, James DE, Yan Z, Hoehn KL. Opening of the mitochondrial permeability transition pore links mitochondrial dysfunction to insulin resistance in skeletal muscle. Molecular metabolism. 2014; 3:124–134. [PubMed: 24634818]
23. Kharel Y, Morris EA, Congdon MD, Thorpe SB, Tomsig JL, Santos WL, Lynch KR. Sphingosine Kinase 2 Inhibition and Blood Sphingosine 1-phosphate Levels. The Journal of pharmacology and experimental therapeutics. 2015

24. Chow JD, Lawrence RT, Healy ME, Dominy JE, Liao JA, Breen DS, Byrne FL, Kenwood BM, Lackner C, Okutsu S, Mas VR, Caldwell SH, Tomsig JL, Cooney GJ, Puigserver PB, Turner N, James DE, Villen J, Hoehn KL. Genetic inhibition of hepatic acetyl-CoA carboxylase activity increases liver fat and alters global protein acetylation. Molecular metabolism. 2014; 3:419–431. [PubMed: 24944901]
25. Billaud M, Lohman AW, Johnstone SR, Biwer LA, Mutchler S, Isakson BE. Regulation of cellular communication by signaling microdomains in the blood vessel wall. Pharmacological reviews. 2014; 66:513–569. [PubMed: 24671377]
26. Igarashi J, Thatte HS, Prabhakar P, Golan DE, Michel T. Calcium-independent activation of endothelial nitric oxide synthase by ceramide. Proceedings of the National Academy of Sciences of the United States of America. 1999; 96:12583–12588. [PubMed: 10535965]
27. Igarashi J, Bernier SG, Michel T. Sphingosine 1-phosphate and activation of endothelial nitric-oxide synthase. differential regulation of Akt and MAP kinase pathways by EDG and bradykinin receptors in vascular endothelial cells. The Journal of biological chemistry. 2001; 276:12420–12426. [PubMed: 11278407]
28. Cantalupo A, Zhang Y, Kothiya M, Galvani S, Obinata H, Bucci M, Giordano FJ, Jiang XC, Hla T, Di Lorenzo A. Nogo-B regulates endothelial sphingolipid homeostasis to control vascular function and blood pressure. Nature medicine. 2015; 21:1028–1037.
29. Oancea E, Meyer T. Protein kinase C as a molecular machine for decoding calcium and diacylglycerol signals. Cell. 1998; 95:307–318. [PubMed: 9814702]
30. Lipp P, Reither G. Protein kinase C: the "masters" of calcium and lipid. Cold Spring Harbor perspectives in biology. 2011; 3
31. Mutchler SM, Straub AC. Compartmentalized nitric oxide signaling in the resistance vasculature. Nitric oxide : biology and chemistry / official journal of the Nitric Oxide Society. 2015; 49:8–15. [PubMed: 26028569]
32. Meens MJ, Alonso F, Le Gal L, Kwak BR, Haefliger JA. Endothelial Connexin37 and Connexin40 participate in basal but not agonist-induced NO release. Cell communication and signaling : CCS. 2015; 13:34. [PubMed: 26198171]
33. Pfenniger A, Derouette JP, Verma V, Lin X, Foglia B, Coombs W, Roth I, Satta N, Dunoyer-Geindre S, Sorgen P, Taffet S, Kwak BR, Delmar M. Gap junction protein Cx37 interacts with endothelial nitric oxide synthase in endothelial cells. Arteriosclerosis, thrombosis, and vascular biology. 2010; 30:827–834.
34. Alonso F, Boittin FX, Beny JL, Haefliger JA. Loss of connexin40 is associated with decreased endothelium-dependent relaxations and eNOS levels in the mouse aorta. American journal of physiology. Heart and circulatory physiology. 2010; 299:H1365–H1373. [PubMed: 20802140]
35. Mather S, Dora KA, Sandow SL, Winter P, Garland CJ. Rapid endothelial cell-selective loading of connexin 40 antibody blocks endothelium-derived hyperpolarizing factor dilation in rat small mesenteric arteries. Circ. Res. 2005; 97:399–407. [PubMed: 16037574]
36. English AR, Zurek N, Voeltz GK. Peripheral ER structure and function. Current opinion in cell biology. 2009; 21:596–602. [PubMed: 19447593]
37. Iwakiri Y, Satoh A, Chatterjee S, Toomre DK, Chalouni CM, Fulton D, Groszmann RJ, Shah VH, Sessa WC. Nitric oxide synthase generates nitric oxide locally to regulate compartmentalized protein S-nitrosylation and protein trafficking. Proceedings of the National Academy of Sciences of the United States of America. 2006; 103:19777–19782. [PubMed: 17170139]
38. Boo YC, Kim HJ, Song H, Fulton D, Sessa W, Jo H. Coordinated regulation of endothelial nitric oxide synthase activity by phosphorylation and subcellular localization. Free radical biology & medicine. 2006; 41:144–153. [PubMed: 16781462]
39. Fleming I, Fisslthaler B, Dimmeler S, Kemp BE, Busse R. Phosphorylation of Thr(495) regulates Ca(2+)/calmodulin-dependent endothelial nitric oxide synthase activity. Circulation research. 2001; 88:E68–E75. [PubMed: 11397791]
40. Sim AT, Scott JD. Targeting of PKA, PKC and protein phosphatases to cellular microdomains. Cell calcium. 1999; 26:209–217. [PubMed: 10643559]

41. Rosse C, Linch M, Kermorgant S, Cameron AJ, Boeckeler K, Parker PJ. PKC and the control of localized signal dynamics. Nature reviews. Molecular cell biology. 2010; 11:103–112. [PubMed: 20094051]
42. Sonkusare SK, Dalsgaard T, Bonev AD, Hill-Eubanks DC, Kotlikoff MI, Scott JD, Santana LF, Nelson MT. AKAP150-dependent cooperative TRPV4 channel gating is central to endothelium-dependent vasodilation and is disrupted in hypertension. Science signaling. 2014; 7:ra66. [PubMed: 25005230]
43. Wang L, Wu B, Sun Y, Xu T, Zhang X, Zhou M, Jiang W. Translocation of protein kinase C isoforms is involved in propofol-induced endothelial nitric oxide synthase activation. British journal of anaesthesia. 2010; 104:606–612. [PubMed: 20348139]
44. Partovian C, Zhuang Z, Moodie K, Lin M, Ouchi N, Sessa WC, Walsh K, Simons M. PKCalpha activates eNOS and increases arterial blood flow in vivo. Circulation research. 2005; 97:482–487. [PubMed: 16081872]
45. Oubaha M, Gratton JP. Phosphorylation of endothelial nitric oxide synthase by atypical PKC zeta contributes to angiopoietin-1-dependent inhibition of VEGF-induced endothelial permeability in vitro. Blood. 2009; 114:3343–3351. [PubMed: 19564638]
46. Haines RJ, Corbin KD, Pendleton LC, Eichler DC. Protein kinase Calpha phosphorylates a novel argininosuccinate synthase site at serine 328 during calcium-dependent stimulation of endothelial nitric-oxide synthase in vascular endothelial cells. The Journal of biological chemistry. 2012; 287:26168–26176. [PubMed: 22696221]
47. Xiao Z, Wang T, Qin H, Huang C, Feng Y, Xia Y. Endoplasmic reticulum Ca2+ release modulates endothelial nitric-oxide synthase via extracellular signal-regulated kinase (ERK) 1/2-mediated serine 635 phosphorylation. The Journal of biological chemistry. 2011; 286:20100–20108. [PubMed: 21454579]
48. Michell BJ, Chen Z, Tiganis T, Stapleton D, Katsis F, Power DA, Sim AT, Kemp BE. Coordinated control of endothelial nitric-oxide synthase phosphorylation by protein kinase C and the cAMP-dependent protein kinase. J. Biol. Chem. 2001; 276:17625–17628. [PubMed: 11292821]
49. Dimmeler S, Fleming I, Fisslthaler B, Hermann C, Busse R, Zeiher AM. Activation of nitric oxide synthase in endothelial cells by Akt-dependent phosphorylation. Nature. 1999; 399:601–605. [PubMed: 10376603]
50. Fulton D, Gratton JP, McCabe TJ, Fontana J, Fujio Y, Walsh K, Franke TF, Papapetropoulos A, Sessa WC. Regulation of endothelium-derived nitric oxide production by the protein kinase Akt. Nature. 1999; 399:597–601. [PubMed: 10376602]
51. Maxfield FR, van Meer G. Cholesterol, the central lipid of mammalian cells. Current opinion in cell biology. 2010; 22:422–429. [PubMed: 20627678]
52. Xu X, London E. The effect of sterol structure on membrane lipid domains reveals how cholesterol can induce lipid domain formation. Biochemistry. 2000; 39:843–849. [PubMed: 10653627]
53. van Meer G, Voelker DR, Feigenson GW. Membrane lipids: where they are and how they behave. Nature reviews. Molecular cell biology. 2008; 9:112–124. [PubMed: 18216768]
54. Miersch S, Espey MG, Chaube R, Akarca A, Tweten R, Ananvoranich S, Mutus B. Plasma membrane cholesterol content affects nitric oxide diffusion dynamics and signaling. The Journal of biological chemistry. 2008; 283:18513–18521. [PubMed: 18445594]

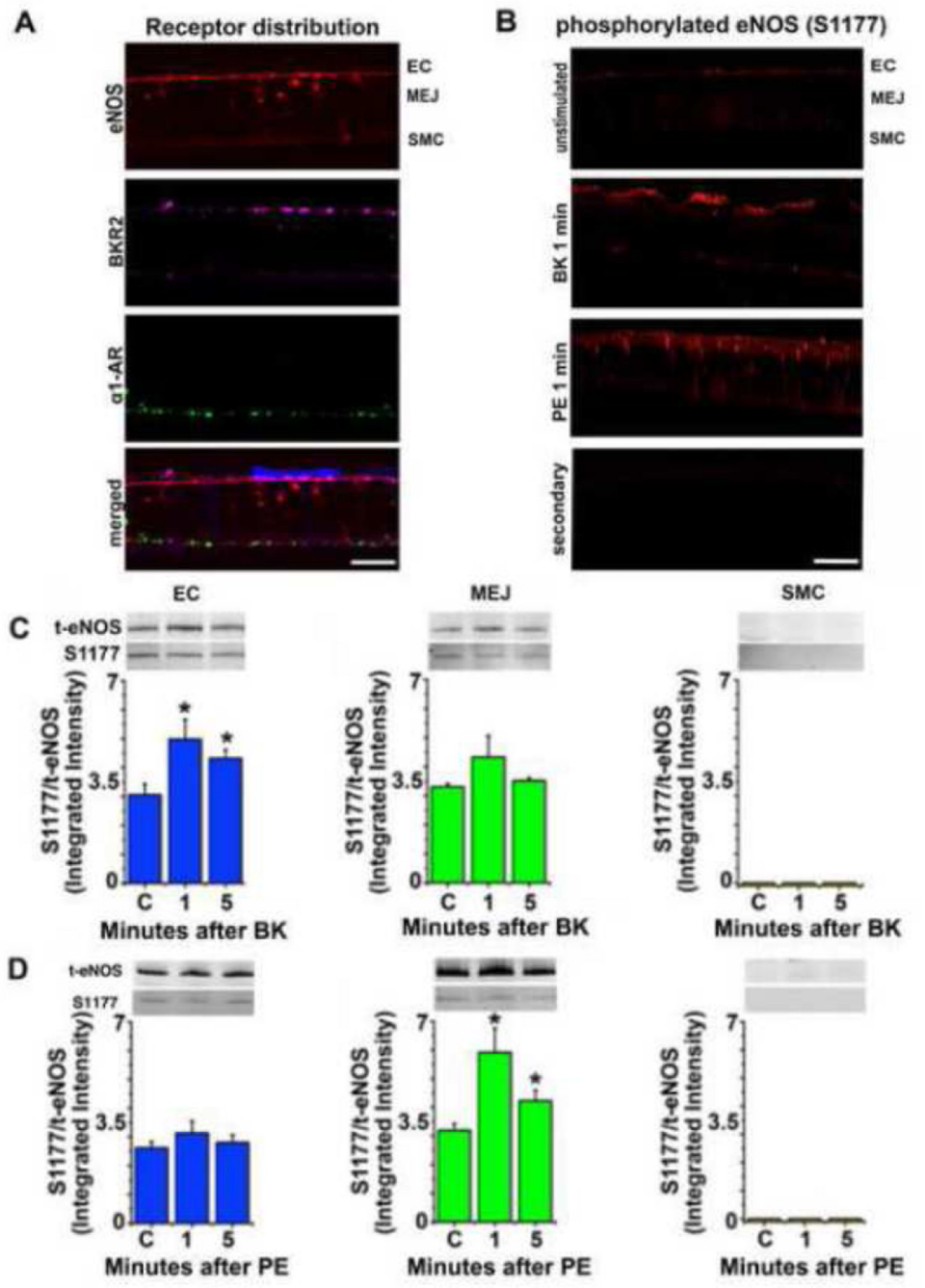

FIGURE 1. Endothelial NOS at serine 1177 is selectively phosphorylated based upon endothelial or smooth muscle cell receptor activation

Transverse sections of the VCCC were incubated with antibodies to alpha 1 adrenergic receptor (α1AR, green), bradykinin receptor 2 (BKR2, purple) and endothelial nitric oxide synthase (eNOS, red). SMC only shows α1AR expression while EC only shows BKR2 expression. Endothelial NOS is found in the apical EC as well as the MEJ (A). Immunocytochemistry of VCCC with antibodies against phosphorylated eNOS at S1177 (eNOS-P, red) after stimulation with BK or PE for 1 minute (B). Representative western blot of VCCC fractions after treatment with bradykinin (BK, 10μM, n=4) (C) or phenylephrine

(PE, 50μM, n=5) (D) at 1 and 5 minute timepoints, with no treatment as control. The ratio of eNOS-P to total eNOS is presented. All error bars represent SEM. In C and D, * indicates $p<0.05$. Scale bar for A and B is 10 μm.

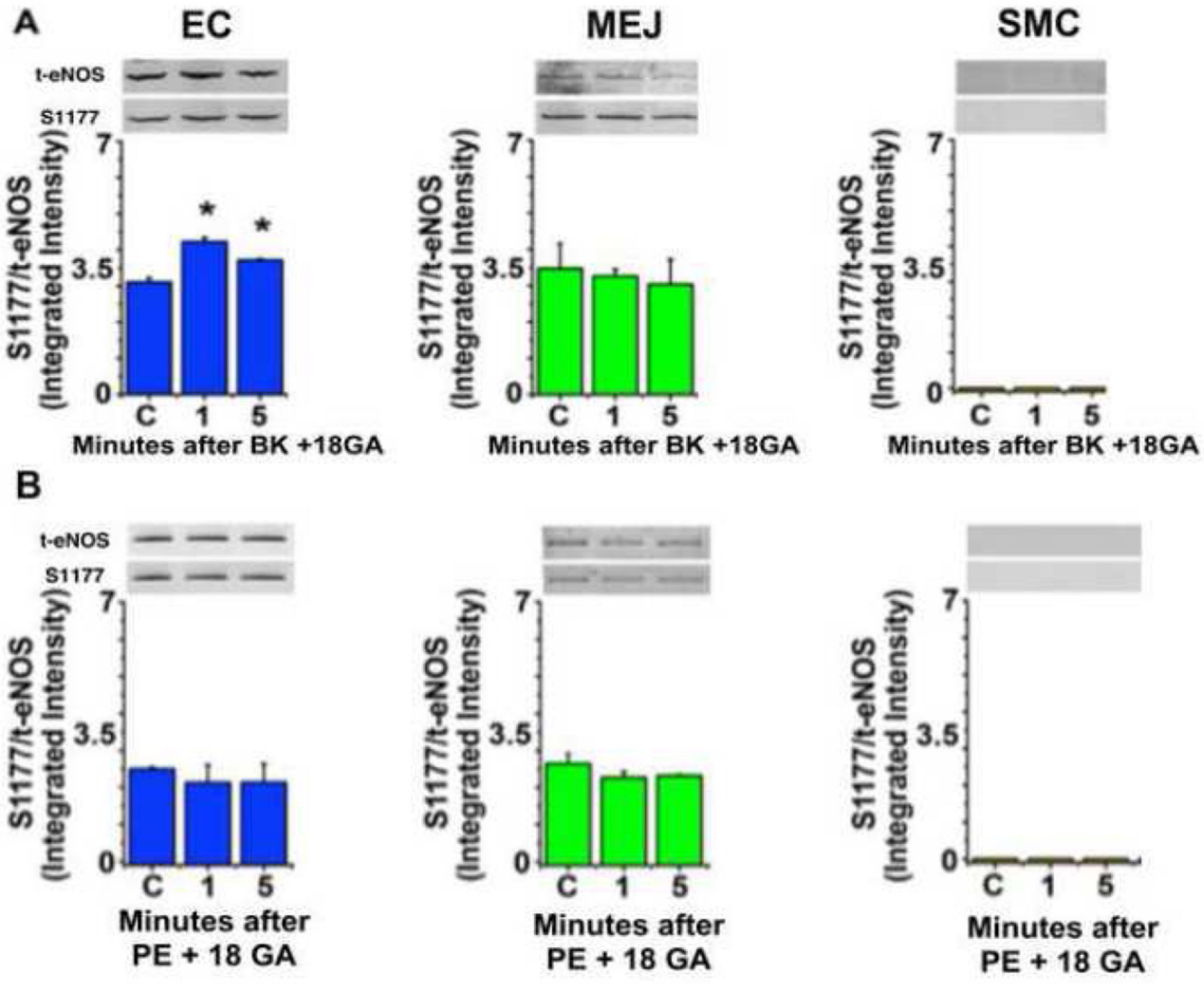

FIGURE 2. Gap junction inhibition prevents phenylephrine induced eNOS phosphorylation at the MEJ

The VCCC was incubated with the gap junction inhibitor 18-GA (50μM) for 30 minutes before adding bradykinin (BK, 10μM, n=4) (A) or phenylephrine (PE, 50μM, n=3) (B). Timepoints indicate the minutes after stimulation. Cellular fractions were harvested for western blotting and the ratio of eNOS S 1177 to total eNOS is presented. All error bars represent SEM. In A and B, * indicates $p<0.05$

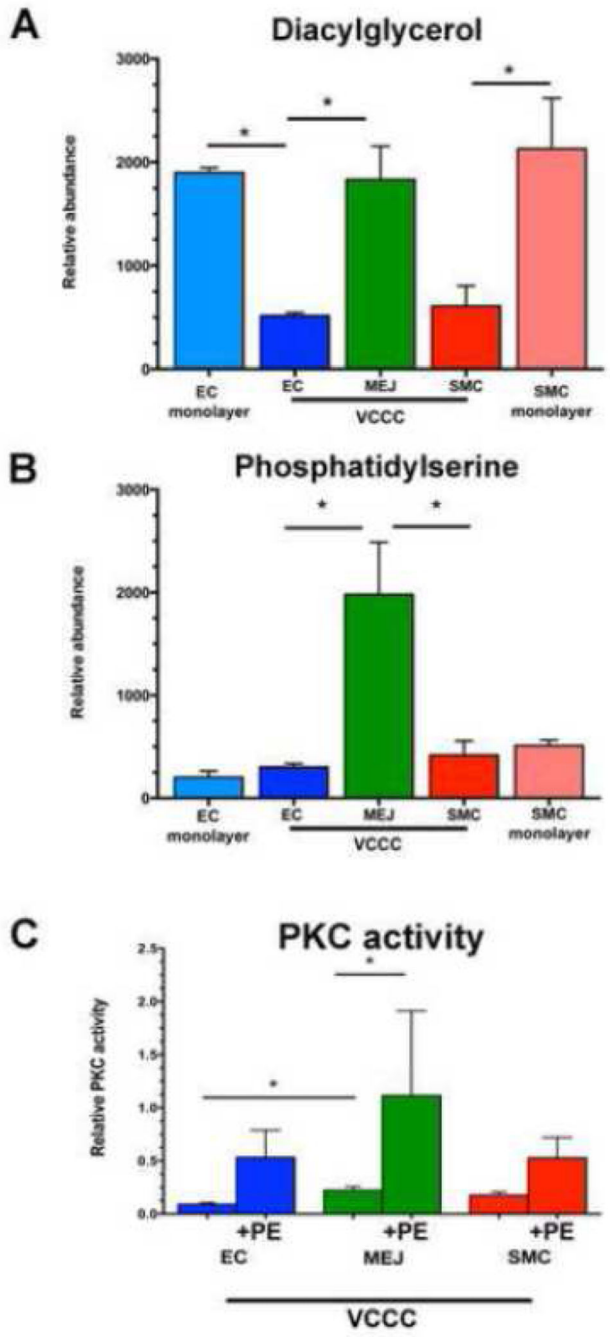

FIGURE 3. Diacylglycerol (DAG) and phosphatidylserine (PS) are enriched at the MEJ, facilitating a significant increase in PKC activity

Glycerolipids (n=3) were isolated from VCCC fractions and EC or SMC monolayers and analyzed via mass spectrometry (A, B). PKC activity measured in the VCCC (n=3) (C). Lipid values were first normalized to an internal standard and then all values were normalized to protein concentration. Error bars represent SEM. * indicates $p<0.05$

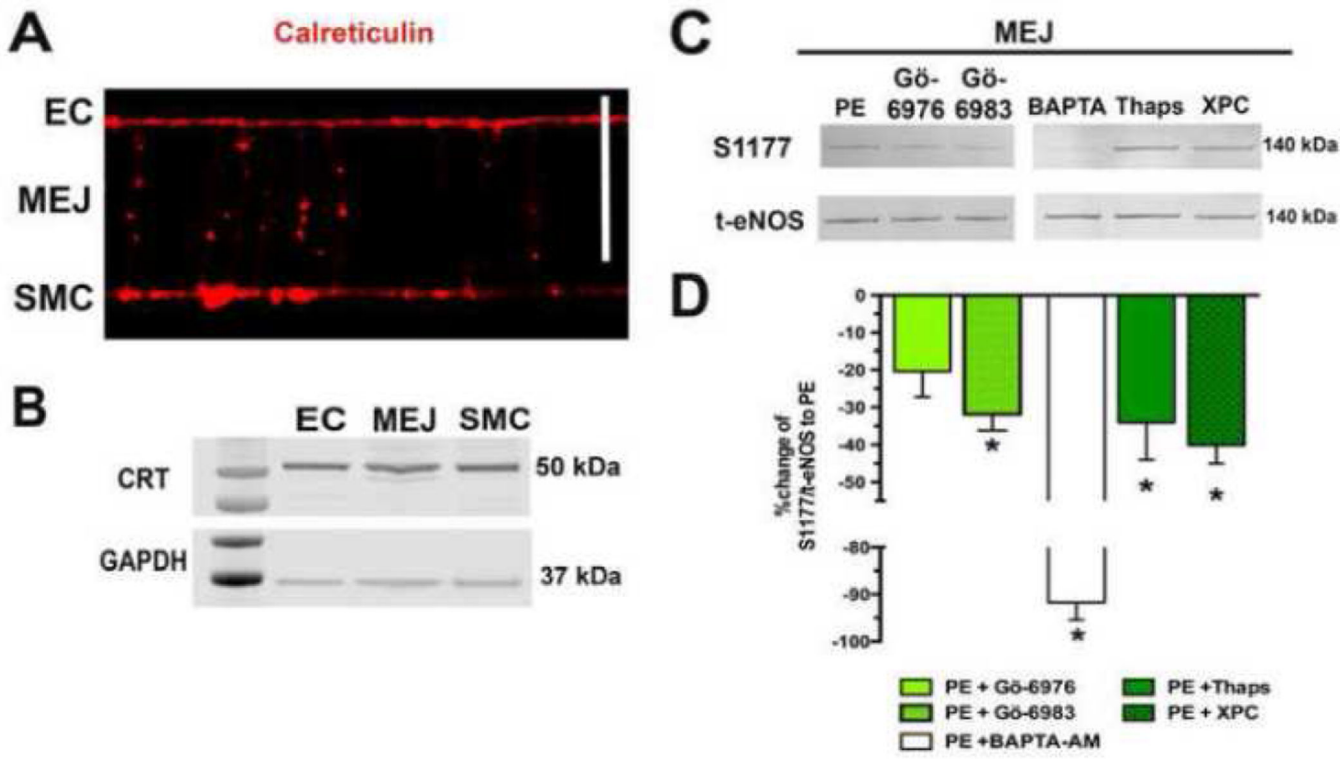

FIGURE 4. Endoplasmic reticulum is present at the MEJ, influencing eNOS phosphorylation

Calreticulin, a class marker of the endoplasmic reticulum, was identified in the VCCC via immunocytochemistry (A) and western blot (B).. Scale bar is 10 mm. Representative eNOS-P to total eNOS blots for MEJ samples after stimulation with PE (50uM, 1 minute, n=3) and incubation with Gö-6976 (10μM, 30 min, n=6), a classical PKC inhibitor, Gö-6983 (10μM, 30 min, n=5), a broad PKC inhibitor, BAPTA (20μM, 20 min, n=4) to chelate calcium, Thapsigargin (2μM, 30 min, n=4) to deplete ER calcium or Xestospongin C (20μM, 10 min, n=3) to inhibit IP_3 receptor signaling (D). The ratio of S1177 to total eNOS was compared back to the PE stimulated ratio (E).

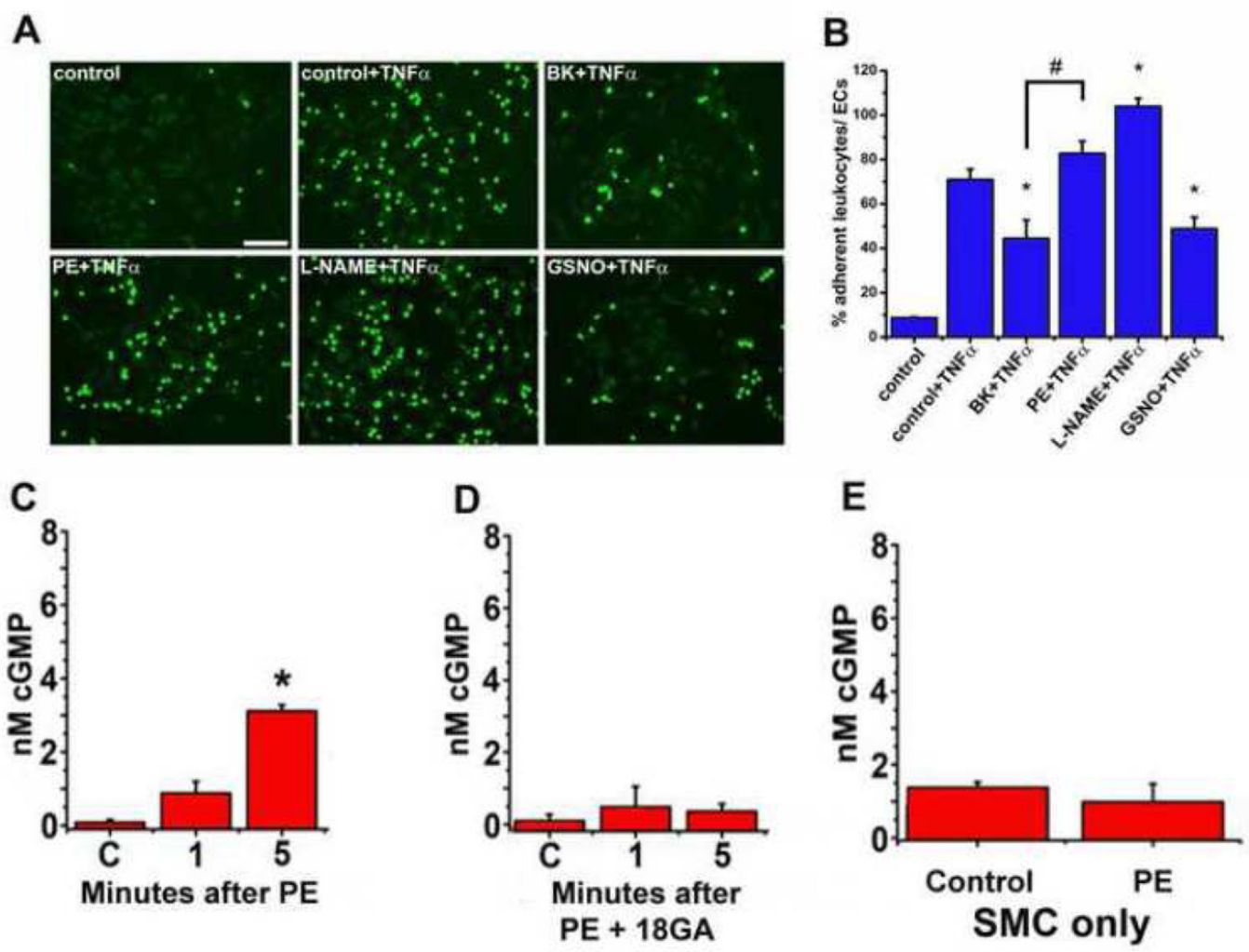

FIGURE 5. Functional effects of apical eNOS versus MEJ eNOS

Representative images of Calcein-AM (5μM) loaded THP1 monocytes (green) adhering to the EC side of the VCCC (A). The VCCC were incubated with TNFα for 4 hours before adding BK (1μM), PE (50μM) or GSNO (100μM) to the EC side for 1 min. A subset of VCCC had L-NAME (100μM) added at the same time as TNFα. Data presented as the percentage of adherent THP1 monocytes to endothelial cells (B). The VCCC were stimulated with phenylephrine (C) or the gap junction inhibitor 18-GA prior to PE stimulation (D). As a control, after SMC were grown in a monolayer they were stimulated with PE and cGMP was measured (E). All error bars represent SEM. B: * indicates $p<0.05$ vs control + TNFα, # indicates $p<0.05$ vs BK + TNFα. C–E: *indicates $p<0.05$ versus control, n=4–6.

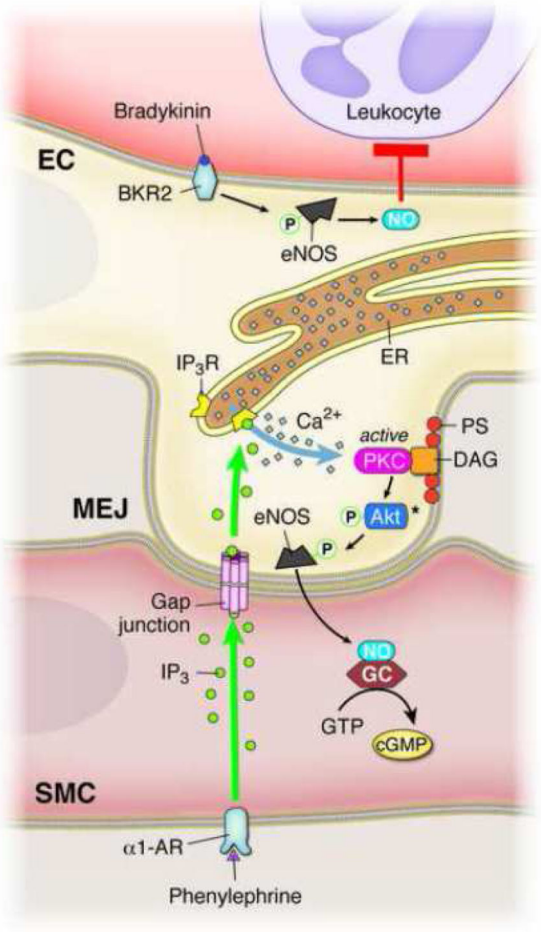

FIGURE 6. Proposed mechanism of differential eNOS phosphorylation in endothelium

Bradykinin activation of the bradykinin receptor 2 (BKR2) causes an increase in eNOS-P in the apical endothelium, leading to significantly decreased leukocyte adhesion via production of anti-inflammatory NO generation. Phenylephrine activation of the α1-AR generates IP_3, which can travel through gap junctions at the MEJ and activate localized IP_3 receptors on the ER. Local ER calcium release contributes to MEJ eNOS-P via activation of MEJ localized PKC, which may occur via Akt. The unique phospholipid composition of the MEJ facilitates this localization of PKC via its lipid cofactors, PS and DAG. Activation of MEJ eNOS with subsequent production of NO leads to increases in SMC cGMP.

TABLE 1

Lipid content of the VCCC and EC or SMC monolayers

Data expressed as the mean relative abundance ± SEM.

	EC monolayer	EC-VCCC	MEJ-VCCC	SMC-VCCC	SMC monolayer
SPHINGOLIPIDS					
Sphinganine	96.886 ± 27.2000	122.363 ± 39.5600	315.932 ± 13.8800 *	91.867 ± 33.5700	99.211 ± 32.8200
Dihydroceramide	4.429 ± 0.4863	11.402 ± 4.0060	5.174 ± 1.6570	3.164 ± 0.4791	6.440 ± 2.0550
Sphingomyelin	209.022 ± 7.1220	78.864 ± 6.5720 **	64.481 ± 21.1800	59.372 ± 16.6700 #	239.757 ± 28.1900
Ceramide	3.903 ± 0.4769	0.0129 ± 0.001867 **	0.0211 ±0.005364	0.0241 ± 0.001354 #	5.423 ± 1.3050
Glucosylceramide	0.872 ± 0.009493	0.735 ± 0.2798	0.942 ± 0.06456	1.122 ± 0.3977	1.033 ± 0.1574
Lactosylceramide	0 ± 0	0.00255 ± 0.001038	0 ± 0	0.000566 ± 0.0005661	1040.530 ± 1041
Sphingosine	22.075 ± 5.9450	11.519 ± 3.2640	14.492 ± 4.4990	4.776 ± 1.7110	18.360 ± 3.2060
Sphingosine 1 Phosphate	0.210 ± 0.04309	0.359 ± 0.1074	0.0314 ± 0.03143 §	0.0902 ± 0.02560	0.0931 ± 0.007039
Dihydro Sphingosine 1 Phosphate	0.0482 ± 0.001834	0 ± 0 **	0 ± 0	0 ± 0 #	0.0724 ± 0.005089
GLYCEROLIPIDS					
Phosphatidylcholine	9.566 ×10^5 ± 3.7102 ×10^4	2.767 ×10^5 ± 2.9548 ×10^4	8.782 ×10^5 ± 3.6615 ×10^5	1.768×10^5 ± 9.9261 ×10^4 #	1.130 ×10^6 ± 2.2572 ×10^5
Phosphatidylethanolamine	4.197 ×10^4 ± 9.5290 ×10^2	6.110 ×10^3 ± 1.1100 ×10^3 **	3.063 ×10^3 ± 9.1370 ×10^2	6.497 ×10^3 ± 6.7360 ×10^2 #	4.457 ×10^4 ± 4.3220 ×10^3
Phosphatidic Acid	63.300 ± 20.3500	140.700 ± 11.5700	1180 ± 216.6000 *	412.700 ± 190.5000	245.300 ± 35.0800
Lysophosphatidic Acid	57.730 ± 4.9890	0 ± 0	0 ± 0	0 ± 0 #	113.900 ± 29.0700
Cholesterol (mg Cho/ug prot)	n/a	33.150 ± 4.7740	17.380 ± 2.4010 §	20.550 ± 3.8770	n/a

* Significant difference ($p<0.05$) as compared to EC and SMC.

** Significant difference as compared to EC monolayer.

\# Significant difference as compared to SMC monolayer.

§Significant difference as compared to EC.